Print ISSN: 2321-6379
Online ISSN: 2321-595X
DOI: 10.17354/ijssl/2017/143

Original Article

Removal of Toluene from Air by Zeolitic Imidazolate Framework-8: Synthesis, Characterization, and Experimental Breakthrough Curve

Saeed Jafari[a], Farshid Ghorbani[*,a], Abdorahman Bahrami[a], Hossein Kazemian[b,c], Saeed Yousefinejad[d]

[a]Center of Excellence for Occupational Health and Research Center for Health Science, School of Public Health, Hamadan University of Medical Sciences, Hamadan, Iran, [b]College of Science and Management, University of Northern British Columbia, Prince George, BC, Canada, [c]Department of Chemical and Biochemical Engineering, Western University, London, ON, Canada, [d]Department of Occupational Health Engeneering, School of Health, Shiraz University of Medical Sciences, Shiraz, Iran

Abstract

Zeolitic imidazolate framework-8 (ZIF-8), a subclass of metal organic frameworks (MOFs), was synthesized from a metal and ligand aqueous solution at room temperature. The samples were characterized by XRD, SEM, and BET, and the results indicated that high purity ZIF-8 crystallites with large surface and micropores volume. The toluene adsorption on the ZIF-8 was studied in a fixed bed reactor. Different pretreatment and activation conditions were examined. Experimental results revealed that adsorption was improved by increasing ZIF-8 pretreatment temperature. Pretreatment conditions were optimized prior to evaluating adsorption efficiency. The effects of toluene concentration, adsorption temperatures and flow rate on experimental breakthrough curves were studied as well. Increasing feed concentration enhances the adsorption capacity, however increasing the adsorption temperature and flow rate decrease the adsorption capacity. The experimental data were fitted with Yan and Thomas models and results showed that these models can describe the experimental breakthrough curve with R square from 92 to 99%. The structure of synthesized ZIF-8 led to different breakthrough behavior at different flow rates of the toluene stream which was discussed in the work as well.

Keywords: Breakthrough curve, Toluene adsorption, Zeolitic imidazolate framework-8

INTRODUCTION

Control of volatile organic compounds (VOCs) emission is very important because of their negative impact on the environment and human health. A wide array of chemical and physical processes such as thermal oxidation, catalytic combustion, biodegradation, adsorption, absorption, condensation, and membrane separation can be utilized for removal of VOCs from contaminated media.[1-4] Adsorption-based technologies are simple, efficient and cost effective processes that can be used for removal and recovery of VOCs even at low concentrations.[5] According to literature, in 2011, merely 10% of industries were using adsorption processes as the main technology to abate exhaust pollutants. However, this trend is increasing because of the implementation of stricter rules and regulations to minimize air release of different pollutants.[6] Various porous materials with high surface area and high pore volume such as activated carbon, zeolites and silica gel are being used as VOCs adsorbent.[7] Among these materials, activated carbon is the most widely used,[3] but it has some disadvantages such as risk of inflammability, deactivation due to its pores clogging and regeneration-related problems.[5]

Recently, Metal Organic Frameworks (MOFs) were recognized as a novel choice in adsorption of various gases and vapors, especially those which are difficult to capture by means of conventional adsorbents[8] owing to their unique properties. MOFs' structure lead to high surface

Access this article online

www.ijss-sn.com

Month of Submission : 04-2017
Month of Peer Review : 05-2017
Month of Acceptance : 06-2017
Month of Publishing : 07-2017

Corresponding Author: F. Ghorban-Shahnai, Tel: 0098-81-38380025, E-mail: fghorbani@umsha.ac.ir

areas, high pore volumes, and mild regeneration condition requirements[9]. MOFs have a variety of basic molecular structures permitting for their pores and functional gropes to be customized for specific applications.[8, 10] All MOFs are composed of metal ligands and organic molecules as linkers, hence, a variety of MOFs can be synthesized.[9-11]

Zeolitic imidazolate frameworks (ZIFs) are a subclass of MOFs where metal ions (e.g., Zn, Co) are linked by imidazolate (e.g., methylimidazolate, ethylimidazolate, etc) to form a unique structure.[12, 13] The ZIFs crystal structure is similar to zeolites except that tetrahedral Si (Al) and bridging oxygen in zeolites is replaced by metal ions and imidazolate link in ZIFs.[14] The angle between metal ions (M) and imidazolate (Im) in the framework structure of ZIFs (M-Im-M) is 145° which is similar to Si-O-Si angle, commonly found in many zeolite topologies.[14-16] The framework structure of ZIFs can be designed to obtain a large spectrum of pore sizes and pore structures. The pore sizes of ZIFs have a wider range in comparison to the pore sizes of zeolites.[17]

So far a large number of ZIFs have been synthesized. ZIF-8 consists of Zn (II) coordinated by four 2-methylimidazolate linkers and has a sodalite topology[12, 18] to compose a 11.5 Å diameter cage connected through 3.4 Å windows.[19] ZIF-8 was first synthesized by Yaghi et al., rhrough a solvothermal method in which zinc nitrate tetrahydrate and 2-methylimidazole were dissolved in dimethylformamide and heated to 140 °C for 24h.[14] In recent years, great efforts have been made to synthesize ZIF-8 in aqueous solutions at room temperature, since organic solvents are flammable and they may cause health and environmental effects. Furthermore, synthesis of ZIF-8 in a facile and environmental friendly method is desirable.[19] Pan et al. first synthesized ZIF-8 in aqueous solution at room temperature with molar ratio of Hmim/Zn equal to about 70.[20] Yao et al. prepared ZIF-8 from stoichiometric Zn and 2-methylimidazol precursor aqueous solutions at room temperature in the presence of Pluronic P123 and ammonium hydroxide.[21] He et al. also prepared ZIF-8 in a concentrated solution of metal and ligand at stoichiometric ratio in the presence of ammonium hydroxide at room temperature.[12]

ZIF-8, as a promising storage material, has been studied by in situ FTIR spectroscopy at high pressures up to ~39 GPa. Structural changes were found to be reversible at low pressure, however structural changes were irreversible at high pressures. Overall, the ZIF-8 framework exhibited an unusual chemical stability even under extreme compression.[22]

ZIF-8 has thermal and chemical stability and is promising for practical applications as gas storage, catalysis and adsorption.[23] Zhu et al. compared the adsorption isotherms of CO_2, CH_4, C_3H_8, and C_3H_6 on ZIF-8 in tablet and powderform, and concluded that the adsorption capacity of these gases on the tablet forms is approximately proportional to the specific surface area loss ratios of the tablet relative to powder.[23] As other application, an enhancement in photocatalytic properties of ZIF-8 loaded TiO_2 nanotubes has been observed for photo-degradation of phenol in a batch reactor.[24]

In the current study, ZIF-8 was synthesized in aqueous solution using an environmentally friendly and cost-effective procedure in aqueous solution at room temperature and was characterized with XRD, SEM, BET. Pretreatment of ZIF-8 was carried out at various temperatures and then toluene dynamic adsorption was measured on the synthesized ZIF-8. The effect of various applied parameters such as temperature of adsorption, flow rate and concentration of toluene on breakthrough curves was also evaluated. In addition, in order to better understand the fixed bed dynamic adsorption of toluene by ZIF-8, the experimental results were fitted with mathematical Yan and Thomas models.

EXPERIMENTAL

Synthesis of Adsorbent

Zinc nitrate hexahydrate [$Zn(NO_3)_2.6H_2O$], 2-methylimidazole (Hmim, $C_4H_6N_2$) and ammonium hydroxide (NH_3, 28–30% aqueous solution, Sigma–Aldrich) were purchased from Sigma–Aldrich, and used without further purification.

Synthesis of ZIF-8 was carried out according to a procedure reported by Yao et al.[21] In a typical process, 1.81 g of $Zn(NO_3)_2.6H_2O$ dissolved in 30 mL of DI (deionized) water. 5.7 g of ammonium hydroxide was added to another 30 mL of DI water and then 2 g of 2-methylimidazole was dissolved in the resulted ammonium hydroxide solution. Finally, 2-methylimidazol solution was added into zinc nitrite solution which immediately obtained a milky suspension mixture. This mixture was mixed at room temperature for 10 min. Synthesized ZIF-8 crystallites were collected by centrifugation at 4000 rpm for 10 min. To wash the product, it was dispersed in 60 ml DI water and centrifuged. Washing was repeated three times. The product was dried at 60 °C overnight in an oven prior to conducting characterization analyses.

Characterization

X-ray diffraction (XRD) was carried out to examine the crystallinity and purity of the products. XRD patterns were measured with a D8 Advance instrument (Cu Kα

radiation) at a scan rate of 2/min with a step size of 0.02 between 5 and 40. Scanning electron microscopy (SEM) images of the samples were obtained by using a Cam Scan Device MV 2300 that operated at 20 kV. Samples were fixed on a conductive carbon double-sided sticky tape and were coated with gold before imaging to reduce the effects of charging. The particle size of ZIF-8 were obtained by Photoshop software from SEM image. The surface area and micropore volume of the ZIF-8 were obtained by measuring the N2 adsorption isotherms at 77 K. Nitrogen adsorption–desorption isotherms were measured by using a Belsorp Mini II. The samples were evacuated for 3 h at 150 °C under vacuum prior to analysis.

The experimental set up

The experimental set up for performing the adsorption of toluene vapor was a continuous flow system. The concentration of toluene vapour was generated with the Evaporation Method.[25] The toluene vapor generator consists of two sections: a toluene container that contains about 20 ml toluene (Merck %99.99) and a mixing chamber. These two sections were connected to each other with a 1 cm internal dimeter and 10 cm long glass tube. The toluene container was placed in a constant-temperature silicon oil bath. The temperature of the bath was adjusted with a PID-type thermostat (Autonics) that was equipped with K-type thermocouple. Dried and pure N2 carrier gas, with a purity of 99.999%, flowed in the mixing chamber. The flow rate of the carrier gas was controlled by mass flow controllers (Alicat Co.) and then merged in the mixing chamber. The quartz tube packed column had a 0.5 cm internal diameter and was 15 cm long. The column was filled with 0.150 g of ZIF-8 and was packed with glass wool. Influent and effluent concentrations were measured with a GC-FID (Varian CP 3800) and the effluent concentration was determined at various times until C/C_0 reached 1.

Measurement of Breakthrough Curves

The toluene adsorption on ZIF-8 was defined by breakthrough curves. The breakthrough curves are expressed in terms of C/C_0 as a function of time (where C and C_0 are the effluent and influent toluene concentrations (mg m^{-3}), respectively). The adsorbed toluene concentration C_{ads} (mg m^{-3}) is equal to $C_0 - C$. The adsorption capacity q (mg g^{-1}) which is the mass of adsorbate per mass of adsorbent m (g) is equal to the area under the curve of the adsorbed toluene concentration C_{ads} versus the time t (min) in a given influent concentration and flow rate Q (m^3 min^{-1}). Furthermore, the following equation can be used to calculate adsorption capacity:[26, 27]

$$q = \frac{Q\int_0^t (C_0 - C)dt}{m} \tag{1}$$

The total adsorption percentage of toluene in the adsorbent was calculated with the following equation that is the ratio of the adsorbed toluene on ZIF-8 s (mg) to the influent total amount of toluene x (mg).[28]

$$A = \frac{s}{x} \times 100 \tag{2}$$

Adsorbent pretreatment

The pretreatment was carried out at various temperatures in a dry air atmosphere. The thermal pretreatment caused the removal of guest molecules (H_2O) or unreacted species (e.g. 2-methylimidazole) from the cavities and the surface of the ZIF-8 crystals.[20] For this reason, 0.15 g of ZIF-8 were packed into the quartz tube and heated in a tubular oven where dry air flowed at 100 mL min^{-1} in the tube. The as-synthesized samples were treated at different temperatures (150°C, 200°C, 250°C, and 300°C for 3 h). After the pretreatment was carried out, dynamic adsorption of each sample was measured separately and the breakthrough curves and adsorption capacity of samples were determined.

Operational parameters evaluation

The effects of carrier gas flow rate of carrier gas, influent concentration of toluene and temperature of adsorbent bed were evaluated on the adsorption capacity, total adsorption percentage, time of breakthrough (C/C_0=0.1), and time of equilibration (C/C_0=0.95). Before any adsorption experiment, pretreatment of all samples was carried out under optimal condition.

Flow rate of carrier gas was set at 20, 50, and 100 mml min^{-1} by mass flow controller. The temperature of silicon oil bath that contained the toluene container was adjusted so that the influent concentration of toluene in influent of adsorbent was constant at 100 ppm. The residence time (t) was calculated with the following equation:[26]

$$t = \frac{\textit{adsorbent bed volume}}{\textit{flow rate}} \tag{3}$$

Concentrations of toluene at 100, 200, and 400 ppm were adjusted as mentioned above and were fed into the quartz tube and then adsorption parameters were determined for each concentration separately. To evaluate the effect of temperature on adsorption, the adsorbents were packed in the quartz tube and were placed into the tubular oven. The temperature of the tubular oven was set at 25, 50, and 80°C and at these conditions, the influent gas with a concentration of toluene of 100 ppm was fed to the quartz tube.

Mathematical Modeling

To interpret the breakthrough curves obtained at different operational conditions, the experimental data was fitted to the mathematical models of Yan and Thomas.[29, 30] Equations (4) and (5) describe Yan and Thomas models respectively:

$$\frac{C}{C_0} = 1 - \frac{1}{1 + \left(\frac{C_0 Q}{q_y m} t\right)^{A_y}} \tag{4}$$

$$\frac{C}{C_0} = \frac{1}{1 + exp\left(\frac{K_T q_T m}{Q} - K_T C_0 t\right)} \tag{5}$$

Where A_y and K_T are Yan and Thomas models' constant respectively; q_y and q_T denote adsorption capacity of adsorbents that have been estimated by Yan and Thomas models. Other parameters are similar to those defined above. To determine fitting parameters such as A_y, K_T, q_y and q_T the experimental data was fitted to the equations (4) and (5). Non-linear least square fitting of the adsorption parameters was done with Levenberg-Marquardt algorithm using MATLAB.

RESULTS AND DISCUSSION

Characterization of the ZIF-8

The XRD pattern of the as-synthesized of ZIF-8, which is illustrated in Fig. 1a, is similar to the simulated XRD Pattern of ZIF-8 [14] with sharp and high-intensities diffraction peaks that indicate phase purity of the synthesized ZIF-8. SEM images are shown in figs. 1b and 1c. The cubic-shape crystallites are characteristic of ZIF-8 crystals. The mean particle size was ~2 μm which is larger than those reported by He et al. (i.e. 0.7 μm). They synthesized ZIF-8 from concentrated aqueous solution of metal and ligand in the presence of ammoniume hydroxide.[12] A small amount of ZIF-8 showed a plate-like shape that resembles the dia topology. Fig. 1d, shows N_2 adsorption-desorption isotherms of as-synthesizeds of ZIF-8 indicating a type I isotherm. The high nitrogen uptake at very low P/P_0 was due to the presence of micropores. BET (Brunauer–Emmet–Teller) surface area and total pore volume were about 847 $m^2 g^{-1}$ and 0.32 $cm^3 g^{-1}$, respectively. This BET surface area is comparable with that reported by Yao et al.[21]

Effect of pretreatment

Fig. 2 shows the effect of pretreatment on the dynamic adsorption of toluene at room temperature, at a constant flow rate (100 mL min^{-1}) of influent gas, an inlet

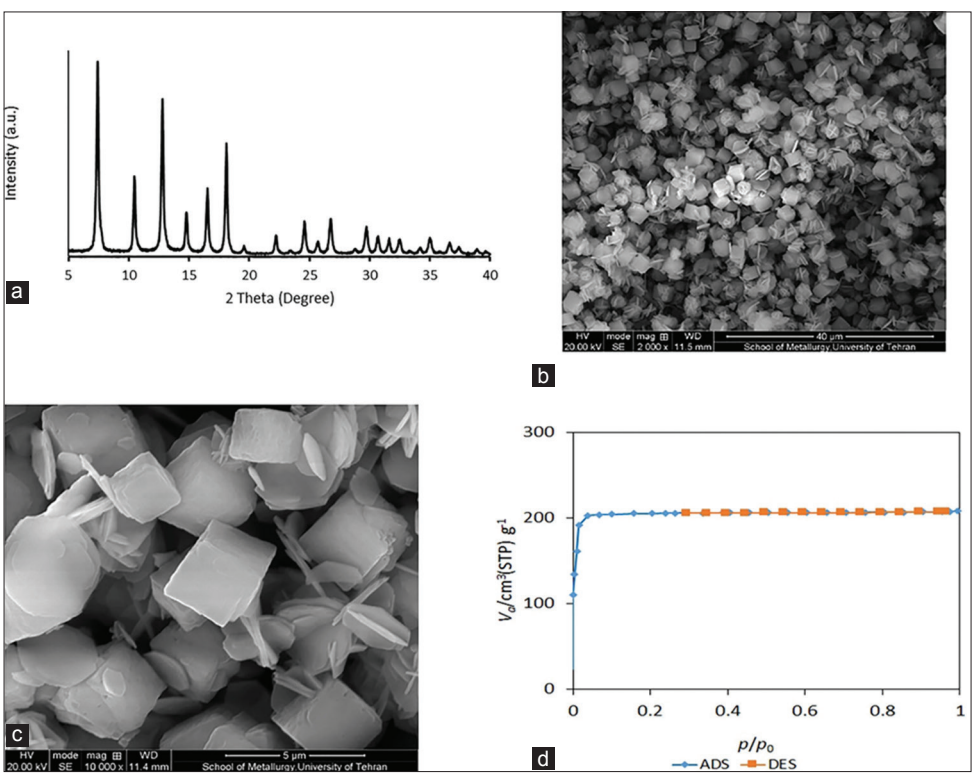

Figure 1. (a) XRD pattern, (b) and (C) SEM micrographs at two different magnifications, and (d) Nitrogen adsorption-desorption of the as-synthesized sample.

concentration of toluene of 100 ppm, a constant ZIF-8 weight of 150 mg, in the same reactor. The adsorption capacity, total adsorption percentage, time of breakthrough, and time of equilibration for different adsorbent are presented in Tab. 1. The rise in the pretreatment temperature affected the operational parameters and the shape of the breakthrough curve, since with increase of pretreatment temperature, the adsorption capacity, total adsorption percent, time of breakthrough, and time of equilibration of samples were increased. The adsorption capacity, time of breakthrough, and time of equilibration of the sample which was pretreated at 300°C for 3h was significantly higher in comparison to other the temperatures.

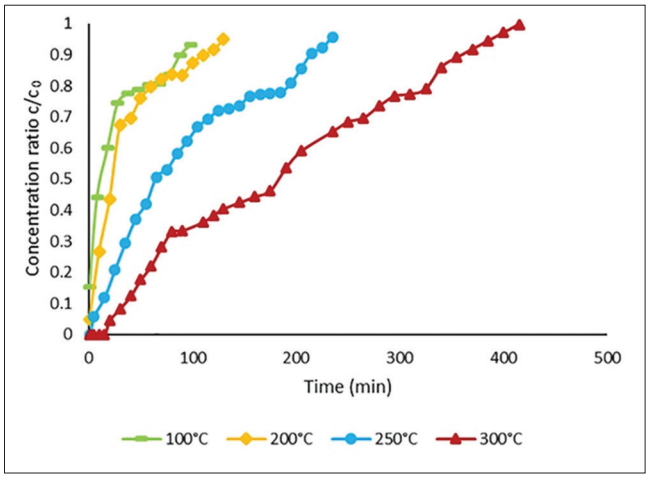

Figure 2. The effects of pretreatment at different temperature on toluene dynamic adsorption on ZIF-8

Pan et al. evaluated the thermal stability of ZIF-8, the samples were stable until 300°C for a duration of 10h and only the color of the samples changed from white to light yellow.[20] The SEM image and XRD pattern of the ZIF-8 after pretreatment and toluene adsorption are shown in the Fig. 3a and 3b. The SEM image did not change in relation to SEM image of as-synthesized ZIF-8 (Fig. 1a), but the XRD pattern changed slightly. Generally, VOCs adsorption on MOF occurs on two sites: organic linkers and metal cations.[26] These results indicate that pretreatment of ZIF-8 at 300°C after 3h can cause the removal of guest molecules and available adsorption sites to take the toluene molecules up.

Flow rate effect

The effect of flow rates 20, 50, 100 mL min^{-1} on toluene adsorption was studied on 0.15 g of ZIF-8 at room temperature with a constant inlet concentration of 100 ppm of toluene in nitrogen carrier gas. Pretreatment of all samples was performed at 300°C for 3h. The breakthrough curve of toluene adsorption at different flow rates is shown in Figs. 4 and 5. The adsorption capacity at 20 and 50 mL min^{-1} were 104 and 47 mg g^{-1}, respectively. Time of breakthrough at 20 and 50 mL min^{-1} were 315 and 50 min, respectively. Time of equilibration at 20 and 50 mL min^{-1} were 845 and 385, respectively. Adsorption capacity, time of breakthrough, and time of equilibration at 100 mL min^{-1} are 41.1 mg g^{-1}, 40 and 385 min, respectively (Tab. 1). These results show that by decreasing the flow rate from 100 mL min^{-1} to 50 mL min^{-1} the adsorption capacity and time of

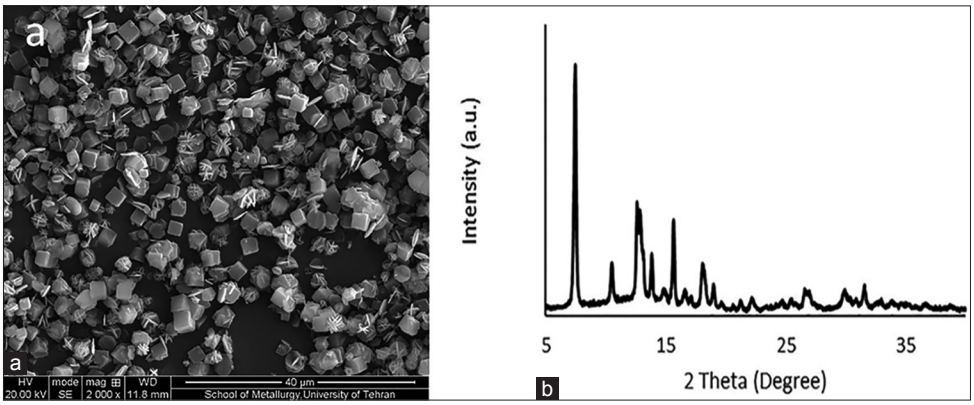

Figure 3. (a) SEM images, and (b) XRD pattern of the ZIF-8 after pretreatment at 300°C for 3h and toluene adsorption

Table 1: The effect of different pretreatment condition on operational parameter of toluene adsorption on ZIF-8

Pretreatment condition	Adsorption capacity (mg g-1)	Total adsorption percentage	Time of breakthrough (min)	Time of equilibration (min)
150°C	5.4	19.45	1	118
200°C	9	25.72	5	130
250°C	21.3	42.84	15	235
300°C	41.1	43.54	40	385

breakthrough slightly increase, but time of equilibration does not change. In relation to these parameters at 100 mL min^{-1}, a decrease in flow rate to 20 mL min^{-1} causes an approximate 2.6, 8, and 2-fold increase in the adsorption capacity, breakthrough time, and equilibration time, respectively. The bed volume of ZIF-8 which packed into the quartz tube was equal to 0.785 cm^3 then the residence time of carrier gas at flow rates of 20, 50, and 100 mL min^{-1} were 2.3, 0.94, and 0.47 seconds, respectively. These results indicate that the residence time had very high effect on adsorption capacity and time of breakthrough of toluene adsorption in microporous of ZIF-8.

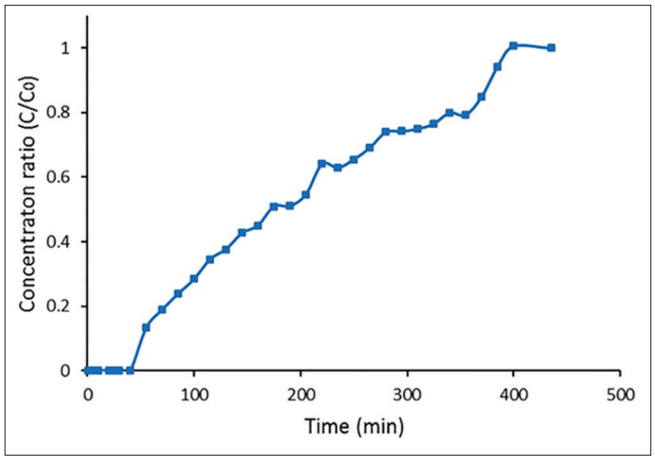

Figure 4. The breakthrough curve of toluene adsorption on ZIF-8 at 50 mL min-1 flow rate of the nitrogen carrier gas

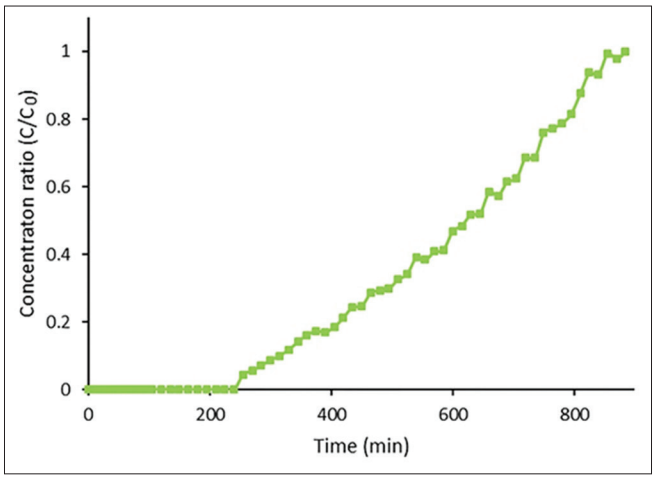

Figure 5. The breakthrough curve of toluene adsorption on ZIF-8 at 20 mL min-1 flow rate of the nitrogen carrier gas

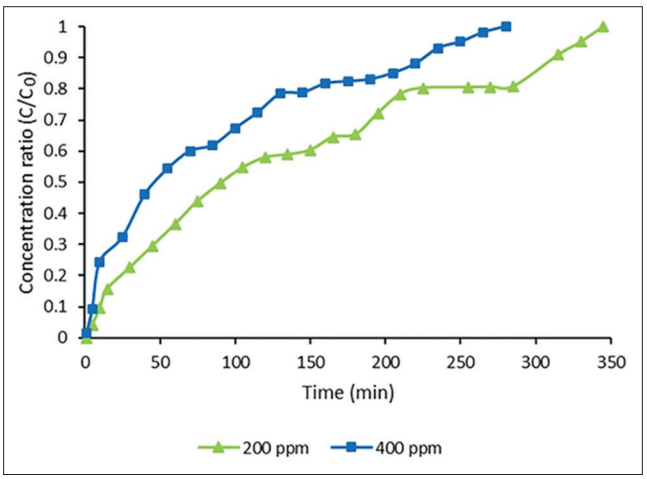

Figure 6. The effects of different concentration of effluent toluene on the breakthrough curve of toluene adsorption on ZIF-8.

Effect of influent concentration

Fig. 6 shows the dynamic adsorption of toluene on ZIF-8 at different concentrations (200, and 400ppm) of toluene in influent gas. The flow rate (100 mL/min), temperature (25°C), weight of adsorbent (0.15g) and configuration of reactor in each experiment was constant. The fig. 6 shows that the rise in concentration affects the breakthrough curve. The adsorption capacity of adsorbent at 200, and 400 ppm were 59.8 and 73.8 mg g^{-1}, respectively. Time of equilibration at 200 and 400 ppm were 330 and 250 min, respectively. The adsorption capacities were higher than the adsorption capacity at 100 ppm, but times of equilibrations decreased at these concentrations in relation to that at 100 ppm (Tab. 1). The time of breakthrough at these concentrations was zero which was less than at 100 ppm (40 min). These results indicate an increase in toluene concentration can increase the mass transfer from gas phase to adsorbent.

Effect of temperature

Fig. 7 shows the breakthrough curves of toluene at different temperatures of adsorption on the ZIF-8. The adsorption capacity of ZIF-8 at 50, and 80°C were 7.9 and 4.2 mg g^{-1}, respectively. Time of equilibration at 50 and 80°C were 160 and 60 min, respectively which was less

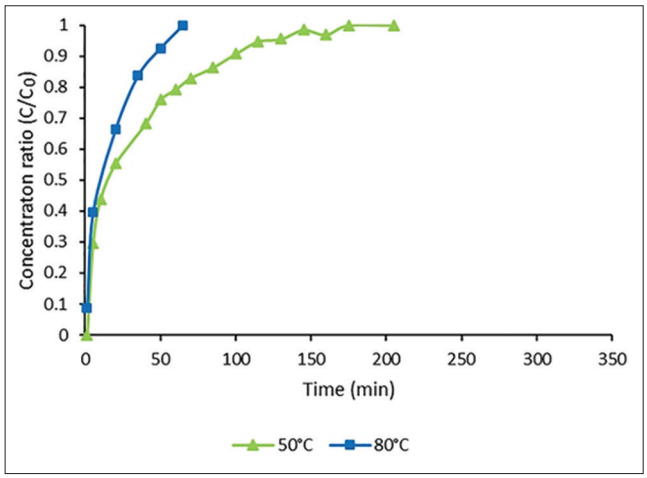

Figure 7. The dynamic toluene adsorption at different bed temperatures on the ZIF-8.

than adsorption at 25°C (Tab. 1). Times of breakthrough at these adsorption temperatures were zero. These results show that by increasing adsorption temperature, adsorption capacity decreases, indicating that adsorption of toluene on ZIF-8 is exothermic.

Curve fitting and description

The experimental curves were fitted with the well-known Yan and Thomas models. The results are presented in Figures 8 to 11. These results indicate that in case of Thomas model when the C/C_0 of experimental results are zero the Y values predicted by model (predicted C/C_0) are not zero and always have a fixed amount which is not in agreement with real conditions i.e. starting from zero values; however, this problem was lower in the Yan model. It should be noted that our findings about the miss-matching the Thomas model in the beginning of the experimental data with y equal to zero are in accordance with previous studies.[29, 30]

As can be seen, predicted breakthrough curves fitted in Yan and Thomas models using non-linear curve fitting have been compared with experimental breakthrough curves of toluene after ZIF-8 pretreatment at 300 °C is shown in Figure 8. The adjusted squared correlation coefficient of the fitting (R^2_{adj}) in Thomas and Yan models were 0.97 and 0.96 respectively which indicate a good of fit. On the other hand, low values of root mean square error (rmse) and sum square error (SSE) in both Thomas and Yan models, equal to 0.06 and 0.11, respectively, confirmed the goodfit of both utilized models for the experimental breakthrough curves at 300 °C. Based on these fittings, the values of q_T in Thomas model and q_y in Yan model were equal to 45.29 and 41.1 mg gr^{-1} respectively which were close to the obtained experimental q (=41.1 mg g^{-1}). Other statistics and predicted parameters are represented in Table 2.

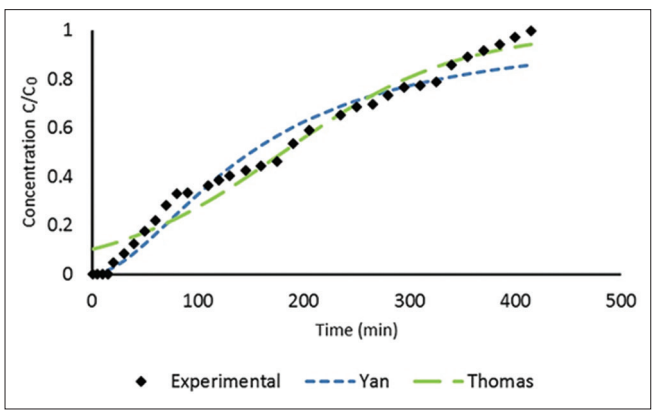

Figure 8. Experimental and predicted breakthrough curves (by non-linear curve fitting) of toluene after ZIF-8 pretreatment at 300 °C.

The breakthrough curves of toluene adsorption at 20 and 50 mL min^{-1} of carrier gas flow rates were fitted with the Yan and Thomas models and are shown in Figs 9(a) and (b). Examining the graphs (Fig 9), it can be seen that Yan and Thomas models are fitted properly to the experimental data at this conditions. Both R^2 and R^2_{adj} in Thomas and Yan models for breakthrough curves of toluene adsorption performed at a carrier gas flow rate equal to 20 mL min^{-1} suggest a near perfect fit. Other fitting statistical parameters (R^2, R^2_{adj}, Rmse and SSE) are listed in Table 2. Despite the good fitting of curves in these conditions with models but the values of q_T in Thomas model and q_y in Yan model were 30.56 and 24.3 mg g^{-1} for the experience done at 20 mL min^{-1} of carrier gas and these values were 24.3 and 21.17 mg g^{-1} for the experience done at 50 mL min^{-1} of carrier gas respectively which were lower than expected from adsorption capacity obtained in actual conditions (=47 and 103 mg g^{-1}).

In continuum of checking the performance of two mathematical models for fitting our obtained breakthrough curves in different conditions, the curves of toluene adsorption at 200 and 400 ppm of influent toluene concentration were fitted with Yan and Thomas models which can be observed in Figs 10 (a) and (b) respectively. Based on the statistical parameters in Table 2, it can be concluded that the curve fits at these conditions are appropriate. Furthermore, the values of q_T in Thomas model and q_y in Yan model were equal to 59.32 and 45.02 mg gr^{-1} respectively for toluene adsorption at 200 ppm which were close to the obtained experimental q (=59.8

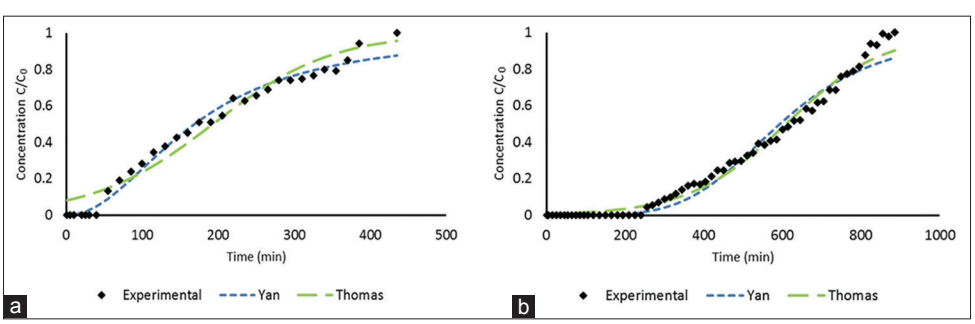

Figure 9. Predicted versus experimental values for adsorption of toluene at (a) 50 and (b) 20 mL min-1 flow rate of carrier gas

mg gr^{-1}). Also during work on the adsorption of toluene with concentration of 400 ppm using Thomas and Yan models, q_T and q_y were 68.01 and 21.15 mg g^{-1} respectively. In comparison to experimental adsorption capacity in this condition (=73.8 mg g^{-1}), the results indicated that Yan model underestimates the adsorption capacity relative to experimental data.

Figures 11 (a) and (b) show the experimental breakthrough curves of the toluene adsorption at bed temperatures of 50 and 80 °C fitted with Yan and Thomas models. The graphs and the values of fitting statistical parameters (R^2, R^2_{adj}, Rmse and SSE) are listed in Table 2 indicated that the experimental results fit properly with Yan and Thomas models as well. As can be seen in Table 2, the estimated q_Y and q_T using curve fitting were close to those obtained experimentally.

In general equation parameters obtained from experimental data fitting of toluene dynamic adsorption

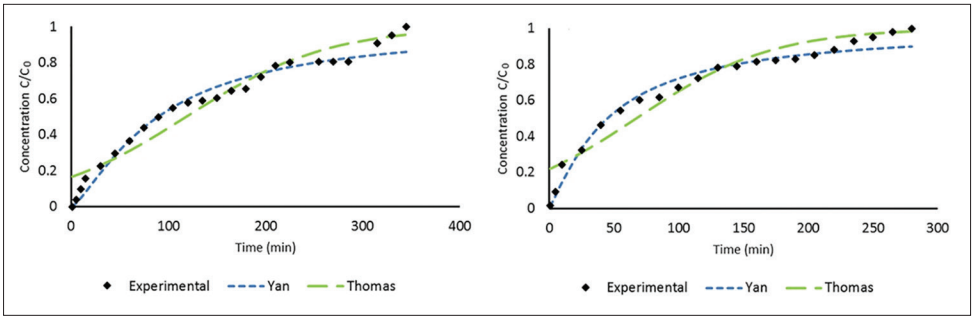

Figure 10. Predicted and experimental breakthrough curves for adsorption of toluene at (a) 200 and (b) 400 ppm influent toluene concentrations

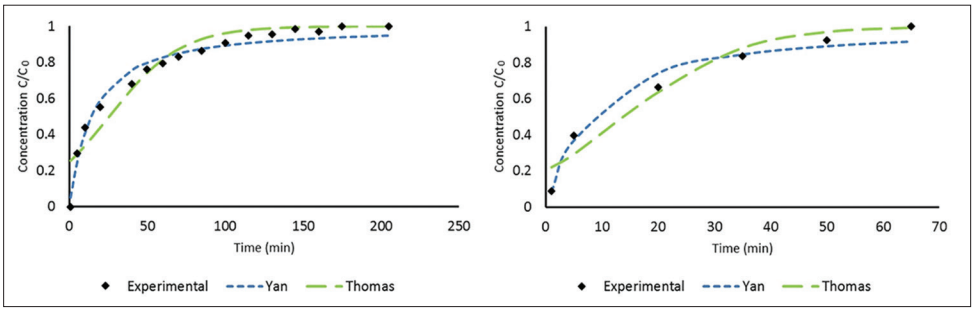

Figure 11. Experimental and predicted breakthrough curves for adsorption of toluene at (a) 50 and (b) 80 °C bed temperature

Table 2: Effect of different operational parameters in Yan and Thomas model parameters for toluene dynamic adsorption on ZIF-8

	Adsorbent Pretreatment (°C)	Flow rate (mL/min)		Concentration ppm		Bed temperature (°C)	
	300	50	20	200	400	50	80
Thomas							
KT	32.04	33.8	21.47	18.11	12.63	114.9	254.8
qT	45.29	24.3	30.56	59.32	68.01	6.47	3.57
R^2	0.967	0.96	0.99	0.94	0.93	0.92	0.95
R^2_{adj}	0.97	0.96	0.99	0.94	0.93	0.91	0.93
Rmse	0.06	0.07	0.04	0.07	0.078	0.09	0.09
SSE	0.11	0.14	0.089	0.12	0.12	0.10	0.03
Yan							
Ay	1.78	2.07	4.59	1.34	1.196	1.1	1.15
qy	37.67	21.17	29.8	45.02	21.15	3.62	2
R^2	0.97	0.98	0.98	0.97	0.97	0.98	0.98
R^2_{adj}	0.96	0.98	0.98	0.97	0.97	0.97	0.97
Rmse	0.06	0.05	0.051	0.05	0.049	0.05	0.06
SSE	0.11	0.07	0.159	0.06	0.045	0.03	0.01
Experimental							
q	41.1	47	104	59.8	73.8	7.9	4.2

on ZIF-8 at different operational parameters with Yan and Thomas mathematical models are listed in Table 2 to make a comparison possible. By looking at the fitting statistical parameters (R^2, R^2_{adj}, Rmse and SSE) total performance of fitting in better sorbents (with resistance to breakthrough) and sorbents with fast breakthrough are almost the same. However, in the cases of 20 and 50 mL min^{-1} flows rate of carrier gas the estimated q_T and q_Y (mg g^{-1}) were less than q valued which were gained experimentally, but in the others operational conditions these values do not differ significantly from the experimental q values (Table 2). Our results showed that by using lower flow rate which leads to more interaction between analyte and sorbents during adsorption, both Thomas and Yan models failed to predict q values accurately for adsorption of toluene on ZIF-8. It could be suggested that increasing the interaction of toluene with the ZIF-8 sorbents in slow flow rate makes the conditions complex and more modified equations are required which is in progress for our future studies.

CONCLUSION

ZIF-8 was synthesized through facile and environmental friendly method. Characterization results and evaluation adsorption efficiency of toluene showed the following:

- The characterization of as-synthesis ZIF-8 showed that pure crystals were formed and the each ZIF-8 crystal size was about 2 μm and surface area and micropore volume were about 847 m^2 g^{-1} and 0.32 cm^3 g^{-1}, respectively.
- Continuous adsorption of toluene in a fixed-bed column was performed by the ZIF-8 adsorbent in various operational conditions. The influence of pretreatment of ZIF-8 adsorbent at various temperatures on the toluene uptake revealed pretreatment of the ZIF-8 from 100°C to 300°C increased adsorption capacities from 5.4 to 41.1 mg g^{-1} respectively.
- Decreasing of flow rate of the toluene-contaminated gas stream from 100 mL min^{-1} to 20 mL min^{-1} increases the adsorption capacity from 104 mg g^{-1} to 41.1 mg g^{-1} respectively.
- Increasing the feed concentration from 100 ppm to 400 ppm increases the adsorption capacity of ZIF-8 from 41.1 mg g^{-1} to 73.8 mg g^{-1}.
- Increasing the temperature of adsorbent bed from 25 °C to 80 °C decreases the adsorption capacity from 41.1 mg g^{-1} to 4.8 mg g^{-1}.
- The experimental breakthrough curves of the adsorption of toluene on were fitted into the Thomas and Yan models with good fitting performance and the q were predicted with both models with good accuracy except while using slow flow rate such as 20 ml/min.

ACKNOWLEDGMENT

The authors would like to thank the Research Consultation Center (RCC) at Shiraz University of Medical Sciences for their invaluable assistance in editing this article.

REFERENCES

1. Qu, F.; Zhu, L.; Yang, K., Adsorption behaviors of volatile organic compounds (VOCs) on porous clay heterostructures (PCH). *J. Hazard. Mater.* 2009, 170, 7-12.
2. Brauer, H.; Varma, Y. B. G., *Air pollution control equipment*. Springer Science & Business Media: 2012.
3. Wang, L. K.; Pereira, N. C.; Hung, Y.-T., *Air pollution control engineering*. Springer: 2004.
4. Seifi, L.; Torabian, A.; Kazemian, H.; Bidhendi, G. N.; Azimi, A. A.; Nazmara, S.; AliMohammadi, M., Adsorption of BTEX on Surfactant Modified Granulated Natural Zeolite Nanoparticles: Parameters Optimizing by Applying Taguchi Experimental Design Method. *CLEAN - Soil, Air, Water*, 2011, 39, 939-948.
5. Zaitan, H.; Bianchi, D.; Achak, O.; Chafik, T., A comparative study of the adsorption and desorption of o-xylene onto bentonite clay and alumina. *J Hazard Mater* 2008, 153, 852-859.
6. Zhao, Z.; Li, X.; Li, Z., Adsorption equilibrium and kinetics of p-xylene on chromium-based metal organic framework MIL-101. *Chem. Eng. J.* 2011, 173, 150-157.
7. Yang, K.; Sun, Q.; Xue, F.; Lin, D., Adsorption of volatile organic compounds by metal-organic frameworks MIL-101: influence of molecular size and shape. *J Hazard Mater* 2011, 195, 124-131.
8. Grant Glover, T.; Peterson, G. W.; Schindler, B. J.; Britt, D.; Yaghi, O., MOF-74 building unit has a direct impact on toxic gas adsorption. *Chem. Eng. Sci.* 2011, 66, 163-170.
9. Mishra, P.; Mekala, S.; Dreisbach, F.; Mandal, B.; Gumma, S., Adsorption of CO2, CO, CH4 and N2 on a zinc based metal organic framework. *Sep. Purif. Technol.* 2012, 94, 124-130.
10. Saha, D.; Deng, S., Ammonia adsorption and its effects on framework stability of MOF-5 and MOF-177. *J Colloid Interface Sci* 2010, 348, 615-20.
11. Saha, D.; Zacharia, R.; Lafi, L.; Cossement, D.; Chahine, R., Synthesis, characterization and hydrogen adsorption on metal-organic frameworks Al, Cr, Fe and Ga-BTB. *Chem. Eng. J* 2011, 171, 517-525.
12. He, M.; Yao, J.; Liu, Q.; Wang, K.; Chen, F.; Wang, H., Facile synthesis of zeolitic imidazolate framework-8 from a concentrated aqueous solution. *Microporous Mesoporous Mater* 2014, 184, 55-60.
13. Cravillon, J.; Münzer, S.; Lohmeier, S.-J.; Feldhoff, A.; Huber, K.; Wiebcke, M., Rapid room-temperature synthesis and characterization of nanocrystals of a prototypical zeolitic imidazolate framework. *Chem. Mater* 2009, 21, 1410-1412.
14. Park, K. S.; Ni, Z.; Cote, A. P.; Choi, J. Y.; Huang, R.; Uribe-Romo, F. J.; Chae, H. K.; O'Keeffe, M.; Yaghi, O. M., Exceptional chemical and thermal stability of zeolitic imidazolate frameworks. *Proc Natl Acad Sci U S A* 2006, 103, 10186-91.
15. Phan, A.; Doonan, C. J.; Uribe-Romo, F. J.; Knobler, C. B.; O'keeffe, M.; Yaghi, O. M., Synthesis, structure, and carbon dioxide capture properties of zeolitic imidazolate frameworks. *Acc. Chem. Res* 2010, 43, 58-67.
16. Banerjee, R.; Phan, A.; Wang, B.; Knobler, C.; Furukawa, H.; O'Keeffe, M.; Yaghi, O. M., High-throughput synthesis of zeolitic imidazolate frameworks and application to CO2 capture. *Science* 2008, 319, 939-943.
17. Liu, Y.; Hu, E.; Khan, E. A.; Lai, Z., Synthesis and characterization of ZIF-69 membranes and separation for CO 2/CO mixture. *J. Membr. Sci* 2010, 353, 36-40.
18. Hertäg, L.; Bux, H.; Caro, J.; Chmelik, C.; Remsungnen, T.; Knauth, M.; Fritzsche, S., Diffusion of CH4 and H2 in ZIF-8. *J. Membr. Sci* 2011, 377, 36-41.
19. Lee, Y.-R.; Jang, M.-S.; Cho, H.-Y.; Kwon, H.-J.; Kim, S.; Ahn, W.-S., ZIF-8: A comparison of synthesis methods. *Chem. Eng. J* 2015, 271, 276-280.
20. Pan, Y.; Liu, Y.; Zeng, G.; Zhao, L.; Lai, Z., Rapid synthesis of zeolitic

imidazolate framework-8 (ZIF-8) nanocrystals in an aqueous system. *Chem Commun* 2011, 47, 2071-2073.
21. Yao, J.; He, M.; Wang, K.; Chen, R.; Zhong, Z.; Wang, H., High-yield synthesis of zeolitic imidazolate frameworks from stoichiometric metal and ligand precursor aqueous solutions at room temperature. *Cryst. Eng. Comm* 2013, 15, 3601-3606.
22. Hu, Y.; Kazemian, H.; Rohani, S.; Huang, Y.; Song, Y., In situ high pressure study of ZIF-8 by FTIR spectroscopy. *Chem Commun* 2011, 47, 12694-12696.
23. Zhu, J.; Jiang, L.; Dai, C.; Yang, N.; Lei, Z., Gas adsorption in shaped zeolitic imidazolate framework-8. *Chin. J. Chem. Eng* 2015, 23, 1275-1282.
24. Isimjan, T. T.; Kazemian, H.; Rohani, S.; Ray, A. K., Photocatalytic activities of Pt/ZIF-8 loaded highly ordered TiO2 nanotubes. *J. Mater. Chem* 2010, 20, 10241-10245.
25. Li, Y.; Täffner, T.; Bischoff, M.; Niemeyer, B., Test Gas Generation from Pure Liquids: An Application-Oriented Overview of Methods in a Nutshell. *Int. J. Chem. Eng* 2012, 1-6.
26. Bahri, M.; Haghighat, F.; Kazemian, H.; Rohani, S., A comparative study on metal organic frameworks for indoor environment application: Adsorption evaluation. *Chem. Eng, J* 2017, 313, 711-723.
27. Yi, H.; Huang, B.; Tang, X.; Li, K.; Yuan, Q.; Lai, R.; Wang, P., Simultaneous Adsorption of SO2, NO, and CO2by K2CO3-Modified γ-Alumina. *Chem. Eng. Technol* 2014, 37, 1049-1054.
28. Zhang, J.; Zhang, X. L.; Li, H.; Zhao, B., Ion Exchange Adsorption Studies of Miglitol in a Fixed Bed. *Chem. Eng. Technol* 2012, 35, 811-818.
29. Yan, G.; Viraraghavan, T.; Chen, M., A new model for heavy metal removal in a biosorption column. *Adsorpt. Sci. Technol* 2001, 19, 25-43.
30. Lima, L. F.; de Andrade, J. R.; da Silva, M. G. C.; Vieira, M. G. A., Fixed Bed Adsorption of BTX Contaminants from Monocomponent and Multicomponent Solutions using a Commercial Organoclay. *Ind. Eng. Chem. Res* 2017, *56*, 6326–6336.

How to cite this article: Jafari S, Ghorbani F, Bahrami A, Kazemian H, Yousefinejad S. Removal of Toluene from Air by Zeolitic Imidazolate Framework-8: Synthesis, Characterization, and Experimental Breakthrough Curve. Int J Sci Stud 2017;5(4):1073-1082.

Source of Support: Nil, **Conflict of Interest:** None declared.